

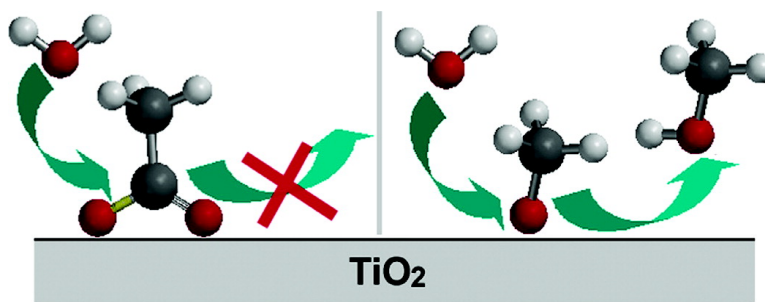
Article

Comparative Study of Acetic Acid, Methanol, and Water Adsorbed on Anatase TiO₂ Probed by Sum Frequency Generation Spectroscopy

Chuan-yi Wang, Henning Groenzin, and Mary Jane Shultz

J. Am. Chem. Soc., **2005**, 127 (27), 9736-9744 • DOI: 10.1021/ja051996m • Publication Date (Web): 22 June 2005

Downloaded from <http://pubs.acs.org> on March 25, 2009



More About This Article

Additional resources and features associated with this article are available within the HTML version:

- Supporting Information
- Links to the 9 articles that cite this article, as of the time of this article download
- Access to high resolution figures
- Links to articles and content related to this article
- Copyright permission to reproduce figures and/or text from this article

[View the Full Text HTML](#)



ACS Publications
 High quality. High impact.

Comparative Study of Acetic Acid, Methanol, and Water Adsorbed on Anatase TiO₂ Probed by Sum Frequency Generation Spectroscopy

Chuan-yi Wang, Henning Groenzin, and Mary Jane Shultz*

Contribution from the Pearson Laboratory, Department of Chemistry, Tufts University, Medford, Massachusetts 02155

Received March 29, 2005; E-mail: Mary.Shultz@tufts.edu

Abstract: Sum frequency generation (SFG) vibrational spectroscopy is used to investigate the surface adsorption of three probe molecules—acetic acid, methanol, and water—on a film composed of nanoscale anatase TiO₂ particles. On the TiO₂ surface, only one adsorption mode, chemisorption, is observed for acetic acid. This is evidenced by one sharp SFG peak in the C–H region, which is stable with time and robust both to evacuation and to the addition of water. A Langmuir constant of $(9.21 \pm 0.71) \times 10^3$ is determined from the adsorption isotherm. In the case of methanol adsorption, however, there are two adsorption modes, molecular physisorption and dissociative chemisorption. The corresponding SFG signals are stable with time but diminished with addition of water. Changes in the SFG features for methanol and for the methoxy species with addition of water and subsequent evacuation provide the first experimental proof of reversible hydroxylation and dehydroxylation at the TiO₂ surface. For water adsorption, only one mode, physisorption, is observed on the hydroxylated TiO₂ surface. The water adlayer is mobile, as is evidenced by variation of the water H-bonded SFG signal with time. Competitive adsorption among the three molecular probes is clearly resolved by in situ SFG measurements. The adsorption strength follows the order acetic acid (strongest), methanol, water (weakest). The adsorption order as well as the difference in response of methanol versus acetic acid adsorption to addition of water has direct implications for understanding TiO₂ photocatalysis as well as the surface modifications involved in TiO₂ photoelectrochemical solar cells and processes in TiO₂ nanomaterial synthesis and assembly.

1. Introduction

In recent years, titanium dioxide (TiO₂) has received considerable attention. This is largely due to its numerous applications in many important fields, such as catalysis, wetting, sensors, corrosion, coatings, and solar cells.^{1–4} All of these applications are initiated by surface and/or interface interactions. To improve the efficacy of materials based on TiO₂, it is thus essential to understand TiO₂ surface chemistry on a molecular level.

TiO₂ primarily exists in three crystalline modifications: rutile, anatase, and brookite. Among the three modifications, rutile and anatase have been extensively studied because of their fundamental and practical interests. Rutile is thermodynamically more stable, while anatase is more widely used in practice, as small particles tend to form as anatase unless annealed at high temperature. Both rutile and anatase are fundamentally made up of [TiO₆] octahedrons, but the modes of arrangement as well

as distortion are different.⁵ In rutile, [TiO₆] octahedrons link by sharing an edge along the *c* axis to form chains, which are further linked by sharing vertices to form a three-dimensional structure. In anatase, the three-dimensional framework is assembled only by edge-shared bonding among the [TiO₆] octahedrons. In view of the different constructions of [TiO₆] octahedrons, the surface chemistry is expected to be significantly different for rutile and anatase. For example, theoretical calculations found that water is molecularly adsorbed on anatase (101),⁶ while on rutile (110) it is dissociatively adsorbed at low coverage.⁷ Most TiO₂ surface studies are conducted in an ultra-high-vacuum (UHV) environment, typically by temperature-programmed desorption (TPD),^{8–11} X-ray photoemission spectroscopy (XPS),^{9,12,13} or low-energy electron diffraction

- (1) Oregan, B.; Grätzel, M. *Nature* **1991**, *353*, 737–740.
- (2) Wang, R.; Hashimoto, K.; Fujishima, A.; Chikuni, M.; Kojima, E.; Kitamura, A.; Shimohigoshi, M.; Watanabe, T. *Nature* **1997**, *388*, 431–432.
- (3) Brown, G. E.; Henrich, V. E.; Casey, W. H.; Clark, D. L.; Eggleston, C.; Felmy, A.; Goodman, D. W.; Grätzel, M.; Maciel, G.; McCarthy, M. I.; Neelson, K. H.; Sverjensky, D. A.; Toney, M. F.; Zachara, J. M. *Chem. Rev.* **1999**, *99*, 77–174.
- (4) Hoffmann, M. R.; Martin, S. T.; Choi, W. Y.; Bahnemann, D. W. *Chem. Rev.* **1995**, *95*, 69–96.

- (5) Wells, A. F. *Structural inorganic chemistry*, 5th ed.; Oxford University Press: New York, 1984.
- (6) Vittadini, A.; Selloni, A.; Rotzinger, F. P.; Grätzel, M. *Phys. Rev. Lett.* **1998**, *81*, 2954–2957.
- (7) Lindan, P. J. D.; Harrison, N. M.; Gillan, M. J. *Phys. Rev. Lett.* **1998**, *80*, 762–765.
- (8) Henderson, M. A.; Epling, W. S.; Peden, C. H. F.; Perkins, C. L. *J. Phys. Chem. B* **2003**, *107*, 534–545.
- (9) Tanner, R. E.; Liang, Y.; Altman, E. I. *Surf. Sci.* **2002**, *506*, 251–271.
- (10) Henderson, M. A. *Surf. Sci.* **1996**, *355*, 151–166.
- (11) Gamble, L.; Hugenschmidt, M. B.; Campbell, C. T.; Jurgens, T. A.; Rogers, J. W. *J. Am. Chem. Soc.* **1993**, *115*, 12096–12105.
- (12) Luo, K.; St Clair, T. P.; Lai, X.; Goodman, D. W. *J. Phys. Chem. B* **2000**, *104*, 3050–3057.
- (13) Diebold, U.; Madey, T. E. *J. Vac. Sci. Technol. A—Vac. Surf. Films* **1992**, *10*, 2327–2336.

(LEED).^{14–17} To date, nearly all the investigations have focused on rutile TiO₂. Rutile (110) is a favorite model system due to its thermodynamic stability and commercial availability in large single crystals. In contrast to the case of rutile, work on anatase has been limited because of the difficulty in preparing suitable large single crystals. Due to recent application of molecular beam epitaxy to growth of anatase TiO₂, UHV studies of anatase single crystals are now possible.^{9,18}

Apart from UHV studies, the TiO₂ surface has also been studied via spectroscopic methods such as FTIR.^{19–21} Recently, the nonlinear vibrational spectroscopic technique sum frequency generation (SFG) coupled with methanol as a molecular probe has been used to study an anatase TiO₂ surface prepared by “wet” chemistry.²² TiO₂ prepared by a wet chemical method is used in photocatalysis and solar cells and so is of widespread practical interest. Characterization of the dependence of methanol adsorption on temperature and pressure provides insight into the nature and properties of the catalytic surfaces such as the surface active sites and the effect of UV irradiation on adsorption.²² The present work probes the competition between acetic acid, water, and methanol.

Study of carboxylic acid adsorption on TiO₂ is relevant to many important processes both in TiO₂-based semiconductor technology and in the catalysis industry. Examples include sensitization of TiO₂ photovoltaic cells to improve solar-to-electric energy conversion efficiency,^{1,23–25} surface passivation and/or modification in nanomaterial synthesis and assembly,^{26–28} and model photoreactions aimed at a mechanistic understanding of TiO₂ photocatalysis.^{28–30} Carboxylic acids have been the subject of many investigations, especially formic acid (HCOOH) adsorption on rutile TiO₂. It has been shown that HCOOH dissociates on oxidized rutile (110).^{31,32} Scanning tunneling microscopy images,^{33,34} X-ray photoelectron diffraction,³⁵ and

ab initio theoretical slab calculations^{19,36} suggest that formate binds to two surface Ti cations in a bridging configuration. Unlike the well-documented case of rutile TiO₂, only limited observations of carboxylic acid adsorption on anatase TiO₂ have been reported. Earlier TPD measurements on anatase powders evidenced both molecular and dissociative adsorption of HCOOH.¹⁹ This is in contrast to the recent results on anatase single crystals. Only dissociative adsorption of carboxylate on anatase TiO₂ (001)^{9,37} is observed by in situ STM, LEED, XPS, and TPD measurements.

Although carboxylic acid adsorption on the TiO₂ surface has been studied for decades, it is not yet well understood. The lack of understanding stems from the need to differentiate trace surface adsorbates from each other, and to separate them from their counterparts in the bulk environment. This is a challenge to traditional spectroscopic methods due to their limited surface sensitivity. In this paper, in situ SFG spectroscopy is used to interrogate these issues.

The theoretical background for SFG is well established in the literature.^{38–40} Within the electric dipole approximation, the sum frequency signal can only be generated where inversion symmetry is broken. Inversion symmetry is necessarily broken at a surface or interface. This inherent advantage renders SFG a prime candidate to probe any surface process, including adsorption, where interference from the bulk phase is undesirable.⁴¹

In addition, compared to a linear vibrational spectroscopy, such as FTIR, more interface molecular information is acquired with SFG because the second-order susceptibility tensor contains more elements. The additional elements enable SFG to determine the molecular conformation at the surface or interface.^{41–43}

The SFG intensity, I_{SFG} , is proportional to the square of the second-order nonlinear susceptibility, $\chi_{\text{ijk}}^{(2)}$.

$$I_{\text{SFG}} \propto \left| \sum_{\text{sum}} L_{\text{sum}} K_{\text{vis}} K_{\text{IR}} \chi_{\text{ijk}}^{(2)} E_{\text{vis}} E_{\text{IR}} \right|^2 \quad (1)$$

where I, J, K is the surface coordinate system, E represents the electric fields at the surface, and K and L are the linear and nonlinear Fresnel coefficients, respectively. The second-order nonlinear susceptibility decomposes into a nonresonant term and a resonant term:

$$\chi^{(2)} = \chi_{\text{NR}}^{(2)} + \chi_{\text{R}}^{(2)} \quad (2)$$

The resonant term $\chi_{\text{R}}^{(2)}$ depends on the density of molecules (N) on the surface and the molecular hyperpolarizability (β) averaged over all molecular orientations on the surface:

$$\chi_{\text{R}}^{(2)} = N \langle \beta \rangle / \epsilon_0 \quad (3)$$

- (14) Tanner, R. E.; Sasahara, A.; Liang, Y.; Altman, E. I.; Onishi, H. *J. Phys. Chem. B* **2002**, *106*, 8211–8222.
 (15) Liang, Y.; Gan, S. P.; Chambers, S. A.; Altman, E. I. *Phys. Rev. B* **2001**, *63*, 235402-1–235402-7.
 (16) Hebenstreit, E. L. D.; Hebenstreit, W.; Diebold, U. *Surf. Sci.* **2000**, *461*, 87–97.
 (17) Herman, G. S.; Sievers, M. R.; Gao, Y. *Phys. Rev. Lett.* **2000**, *84*, 3354–3357.
 (18) Herman, G. S.; Dohnalek, Z.; Ruzycski, N.; Diebold, U. *J. Phys. Chem. B* **2003**, *107*, 2788–2795.
 (19) Rotzinger, F. P.; Kesselman-Truttman, J. M.; Hug, S. J.; Shklover, V.; Grätzel, M. *J. Phys. Chem. B* **2004**, *108*, 5004–5017.
 (20) Nakamura, R.; Imanishi, A.; Murakoshi, K.; Nakato, Y. *J. Am. Chem. Soc.* **2003**, *125*, 7443–7450.
 (21) Baraton, M. I.; Merhari, L. *Nanostruct. Mater.* **1998**, *10*, 699–713.
 (22) Wang, C. Y.; Groenzin, H.; Shultz, M. J. *J. Phys. Chem. B* **2004**, *108*, 265–272.
 (23) Kim, Y. G.; Walker, J.; Samuelson, L. A.; Kumar, J. *Nano Lett.* **2003**, *3*, 523–525.
 (24) Nazeeruddin, M. K.; Kay, A.; Rodicio, I.; Humphrybaker, R.; Muller, E.; Liska, P.; Vlachopoulos, N.; Grätzel, M. *J. Am. Chem. Soc.* **1993**, *115*, 6382–6390.
 (25) Hara, K.; Horiuchi, H.; Katoh, R.; Singh, L. P.; Sugihara, H.; Sayama, K.; Murata, S.; Tachiya, M.; Arakawa, H. *J. Phys. Chem. B* **2002**, *106*, 374–379.
 (26) Rammal, A.; Brisach, F.; Henry, M. C. R. *Chim.* **2002**, *5*, 59–66.
 (27) Venz, P. A.; Klopogge, J. T.; Frost, R. L. *Langmuir* **2000**, *16*, 4962–4968.
 (28) Lawless, D.; Kapoor, S.; Meisel, D. *J. Phys. Chem.* **1995**, *99*, 10329–10335.
 (29) Villarreal, T. L.; Gomez, R.; Neumann-Spallart, M.; Alonso-Vante, N.; Salvador, P. *J. Phys. Chem. B* **2004**, *108*, 15172–15181.
 (30) Ikeda, S.; Sugiyama, N.; Pal, B.; Marci, G.; Palmisano, L.; Noguchi, H.; Uosaki, K.; Ohtani, B. *Phys. Chem. Chem. Phys.* **2001**, *3*, 267–273.
 (31) Uetsuka, H.; Henderson, M. A.; Sasahara, A.; Onishi, H. *J. Phys. Chem. B* **2004**, *108*, 13706–13710.
 (32) Onishi, H.; Aruga, T.; Iwasawa, Y. *J. Am. Chem. Soc.* **1993**, *115*, 10460–10461.
 (33) Sayago, D. I.; Polcik, M.; Lindsay, R.; Toomes, R. L.; Hoefft, J. T.; Kittel, M.; Woodruff, D. P. *J. Phys. Chem. B* **2004**, *108*, 14316–14323.
 (34) Onishi, H.; Iwasawa, Y. *Chem. Phys. Lett.* **1994**, *226*, 111–114.

- (35) Thevuthasan, S.; Herman, G. S.; Kim, Y. J.; Chambers, S. A.; Peden, C. H. F.; Wang, Z.; Ynzunza, R. X.; Tober, E. D.; Morais, J.; Fadley, C. S. *Surf. Sci.* **1998**, *401*, 261–268.
 (36) Kackell, P.; Terakura, K. *Surf. Sci.* **2000**, *461*, 191–198.
 (37) Altman, E. I.; Tanner, R. E. *Catal. Today* **2003**, *85*, 101–111.
 (38) Shen, Y. R. *Nature* **1989**, *337*, 519–525.
 (39) Hirose, C.; Akamatsu, N.; Domen, K. *Appl. Spectrosc.* **1992**, *46*, 1051–1072.
 (40) Bain, C. D. *J. Chem. Soc., Faraday Trans.* **1995**, *91*, 1281–1296.
 (41) Shultz, M. J.; Baldelli, S.; Schnitzer, C.; Simonelli, D. *J. Phys. Chem. B* **2002**, *106*, 5313–5324.
 (42) Simonelli, D.; Shultz, M. J. *J. Chem. Phys.* **2000**, *112*, 6804–6816.
 (43) Richmond, G. L. *Chem. Rev.* **2002**, *102*, 2693–2724.

where ϵ_0 is the permittivity of free space. Within the electric dipole approximation, β can be expressed as^{44,45}

$$\beta_{q,lmn} = \frac{\alpha_{q,lm} \mu_{q,n}}{2\hbar(\omega_q - \omega_{IR} - i\Gamma_q)} \quad (4)$$

where $\alpha_{q,lm}$, $\mu_{q,n}$, ω_q , ω_{IR} , and Γ_q are the Raman tensor element, IR transition dipole moment, resonant frequency, frequency of the IR beam, and the damping constant of the q th molecular vibrational mode, respectively. These SFG characteristics are used for spectral data fitting and quantitative analysis.

In the present work, in situ SFG is applied for the first time to follow the adsorption isotherm of acetic acid on the nanoparticulate TiO₂ film surface. In addition, the competitive adsorption among acetic acid, methanol, and water is further resolved. Interestingly, it is found that acetic acid adsorption is nearly unaffected by the presence of water, while methanol/methoxy adsorption involves reversible hydroxylation/dehydroxylation when water is present.⁴⁶ Competitive adsorption is an omnipresent issue in catalysis, and resolving the issue is of practical significance. The finding of different effects for water competition with acetic acid and with methanol adsorption sheds light on TiO₂ photocatalysis and its surface modification for many important applications, including photoelectrochemical solar cells and nanomaterial synthesis and assembly.

2. Experimental Section

The procedure for the preparation of TiO₂ nanoparticles and fabrication of them into films has been reported elsewhere.²² Briefly, TiO₂ nanoparticles were prepared by controlled hydrolysis of TiCl₄ in water at 0 °C. The resulting colloidal solution was dialyzed for purification and adjustment of pH. Following vacuum rotary evaporation of the colloidal solution at room temperature, powdered samples were finally obtained. As characterized by TEM and HRTEM, the average size of the prepared TiO₂ particles is ca. 2.4 nm with an anatase crystal structure.⁴⁷

TiO₂ films were prepared through an evaporation-driven self-assembly process. A desired amount of the powdered TiO₂ nanoparticles, prepared as described above, was dissolved into water to form a transparent solution. The solution was then dropped onto a clean substrate and left in air to dry. A virtually transparent, continuous film was thus formed. The surface of the prepared TiO₂ film was cleaned, when necessary, by UV irradiation, which was achieved by means of a 1000-W ozone-free xenon lamp (Oriol Instruments) equipped with a 10-cm water filter to eliminate IR radiative heating. A hydrocarbon-free film is verified by a lack of C–H resonances in the SFG spectrum prior to molecular probing.⁴⁸

A TiO₂ film deposited on a CaF₂ substrate was employed in the SFG experiments. The film thickness is ca. 500 nm, as determined by a profilometer (SLOAN DEK TAK). AFM characterization showed that the film surface is flat, with a root-mean-square (RMS) roughness of ± 0.5 nm on a macroscopic scale, enabling efficient collection of the SFG signal.²² The CaF₂ substrate, serving as a window, was mounted on an O-ring-sealed glass cell with the surface-deposited TiO₂ film facing the inside of the cell. The visible and infrared beams used to generate SFG passed from the top side through the window/substrate

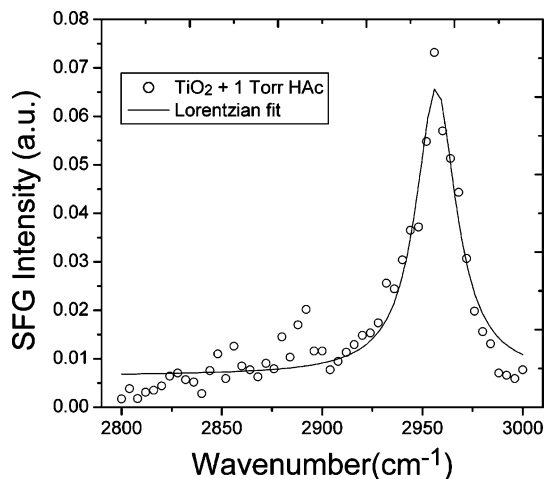


Figure 1. SFG spectrum of acetic acid on a TiO₂ film.

and the film. Potential SFG interference from the top CaF₂–air interface is excluded by spatial filtering. Nonresonant SFG from TiO₂ is weak, and any organic contaminants trapped in the film are removed by UV pre-irradiation, as stated above. The cell was attached to a vacuum line and evacuated by a diffusion pump. After evacuation, the cell was filled with the desired vapor pressure of the probe molecules, including acetic acid, methanol, water, or a mixture of them.

The sum frequency is generated by temporally and spatially overlapping a 532-nm visible and a tunable IR beam on the TiO₂ film surface at incident angles of 50° and 60°, respectively, relative to the surface normal. A more detailed description has been reported elsewhere.⁴⁸ The SFG signal from the sample surface was collected in reflection by a photomultiplier tube after filtering by a polarizer and monochromator. The IR input energy was monitored during the experiment by an energy meter (Moletron J8LP + ENERGY MAX500). The vibrational spectrum from the surface was normalized to the input beam intensities and referenced to the signal from silver. Each data point, taken at a resolution of 4 cm⁻¹, was averaged over 3000 pulses with a gated integrator (Stanford Research Systems, SR250) and stored in a personal computer. For all the SFG measurements, beam polarizations are *s*, *s*, *p* for sum frequency, visible, and infrared, respectively.

3. Results

3.1. Adsorption of Acetic Acid on TiO₂. As described in the Experimental Section, the TiO₂ film is grown “bottom-up” on a substrate so isotropic symmetry is broken at the top layer of the film. Due to the asymmetric environment, molecules adsorbed on the film surface adopt a preferred polar orientation with respect to the surface normal. This preferred orientation gives rise to a characteristic SFG signal.

A representative SFG spectrum in the 2800–3000 cm⁻¹ region, commonly called the C–H stretch region, for gaseous acetic acid adsorbed on TiO₂ is shown in Figure 1. In this region only one sharp peak at ~ 2950 cm⁻¹ appears, attributed to a C–H stretch, indicating that there is only one mode for acetic acid adsorbed on TiO₂. This is much different than the previous observation for methanol adsorption on TiO₂, where two pairs of C–H stretch peaks are observed, suggesting two adsorption modes.²²

The SFG intensity is related to the square of the molecular density on the surface (eqs 1–3). Therefore, any change in surface adsorbance of acetic acid can be monitored by following the C–H stretch peak intensity. The SFG spectral evolution of acetic acid adsorbed on TiO₂ as a function of acetic acid partial

(44) Bell, G. R.; Bain, C. D.; Ward, R. N. *J. Chem. Soc., Faraday Trans.* **1996**, *92*, 515–523.

(45) Guyot-Sionnest, P.; Superfine, R.; Hunt, J. H.; Shen, Y. R. *Chem. Phys. Lett.* **1988**, *144*, 1–5.

(46) Wang, C. Y.; Groenzin, H.; Shultz, M. J. *J. Am. Chem. Soc.* **2004**, *126*, 8094–8095.

(47) Wang, C.-Y.; Böttcher, C.; Bahnmann, D. W.; Dohrmann, J. K. *J. Mater. Chem.* **2003**, *13*, 2322–2329.

(48) Wang, C. Y.; Groenzin, H.; Shultz, M. J. *Langmuir* **2003**, *19*, 7330–7334.

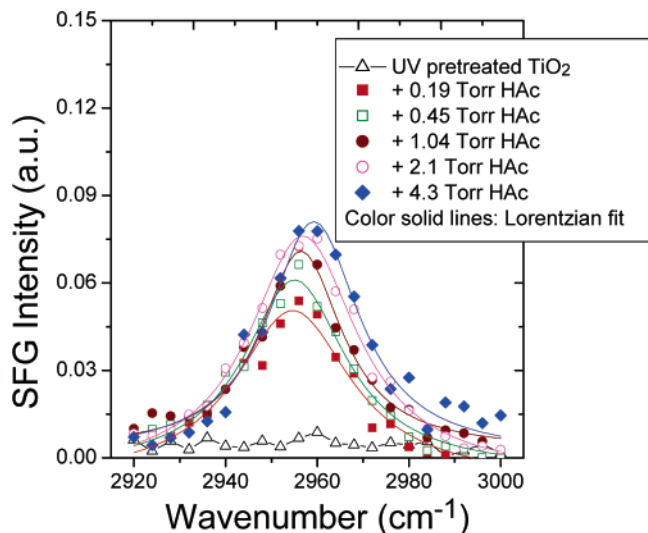


Figure 2. SFG spectral evolution of acetic acid on TiO₂ as a function of vapor pressure.

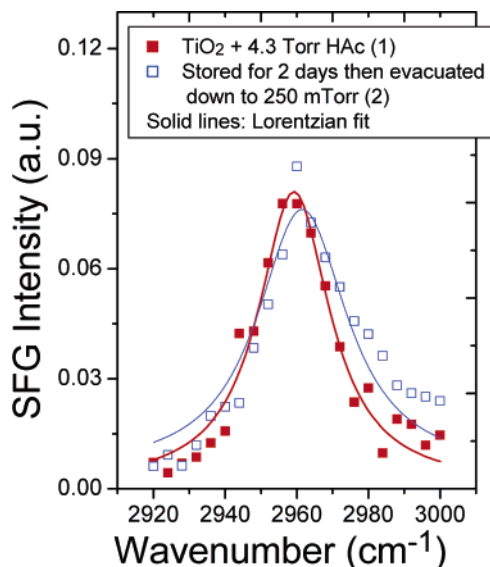


Figure 3. SFG spectra of acetic acid adsorbed on TiO₂ over time and upon evacuation.

pressures is shown in Figure 2. Note that at the highest acetic acid pressure, a spectral “tail” due to H-bonded OH groups results in an apparent peak shift to higher wavenumbers. The data in Figure 2 are used to derive the adsorption isotherm. The isotherm is discussed in section 4.1.

Surface adsorption is generally divided into two categories: physisorption and chemisorption.⁴⁹ The former is mobile, while the latter is relatively stable. The relative adsorption strength for acetic acid on TiO₂ is determined by monitoring changes in the C–H stretch SFG peak with time as well as with evacuation. As can be seen from the spectra in Figure 3, the SFG peak is unchanged over 2 days with the sample evacuated to 250 mTorr. This suggests that acetic acid is relatively strongly adsorbed on the TiO₂ surface. Note that the apparent peak shift and spectral asymmetry observed when the system is stored over 2 days are due to the H-bonded tail, as noted above for Figure 2.

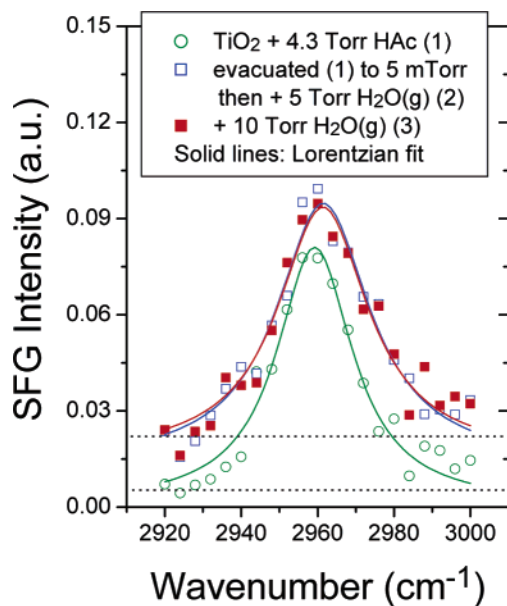


Figure 4. SFG spectra of acetic acid on the TiO₂ surface with addition of water.

The strength of acetic acid adsorption on the TiO₂ surface is further verified by the effect of water on the acetic acid SFG signal. Figure 4 shows the SFG spectra of acetic acid on the TiO₂ surface in the presence of different partial pressures of water. The absorption frequency, bandwidth, and intensity are unaltered upon addition of water except that the baseline is lifted due to the tail of the H-bonded water molecules in the adlayers. This indicates that water has little effect on the adsorption of acetic acid on the TiO₂ surface, supporting the conclusion that acetic acid is more strongly adsorbed on the TiO₂ surface than is water. If acetic acid were less strongly adsorbed, the adsorption equilibrium would be shifted upon addition of excess water, leading to a decrease in the C–H stretch signal intensity, as is observed, e.g., with methanol and water.⁴⁶

3.2. Methanol on TiO₂. In previous work, methanol adsorbed on TiO₂ was characterized with in situ SFG spectroscopy.²² Monitoring the methyl group SFG features as a function of temperature and pressure reveals the methanol surface adsorption characteristics. Methanol adsorbs to TiO₂ in two adsorption modes: physisorbed as molecular methanol and chemisorbed as a methoxy species. The adsorption isotherm and the adsorption temperature dependence confirm these adsorption mode assignments.

For methanol on TiO₂, there are two pairs of C–H stretch peaks, ascribed to a methoxy species (2828 and 2935 cm⁻¹) and molecular methanol (2855 and 2968 cm⁻¹), respectively. Detailed assignment of these peaks has been reported previously.²² Like the acetic acid adsorption, the adsorption of methanol on TiO₂ is stable with time, as is shown by the data in Figure 5.

In contrast to acetic acid, the methanol peaks change upon addition of water. When a large amount of water is present in the system, as shown by the spectra in Figure 6, both the methoxy species and the methanol SFG signals are substantially suppressed. Figure 6b shows the relative change in the methoxy species SFG intensity with various water partial pressures. The methoxy species SFG signal is restored to some extent (Figure

(49) Adamson, A. W. *Physical chemistry of surfaces*, 5th ed.; Wiley: New York, 1990.

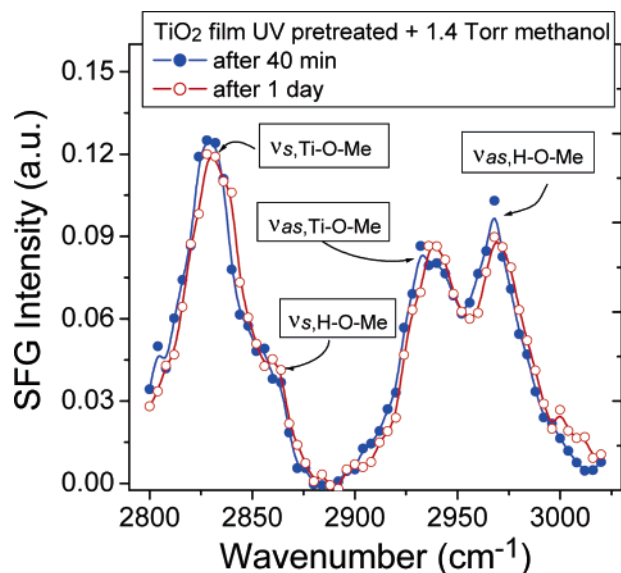


Figure 5. Time-resolved SFG spectra of methanol on TiO₂.

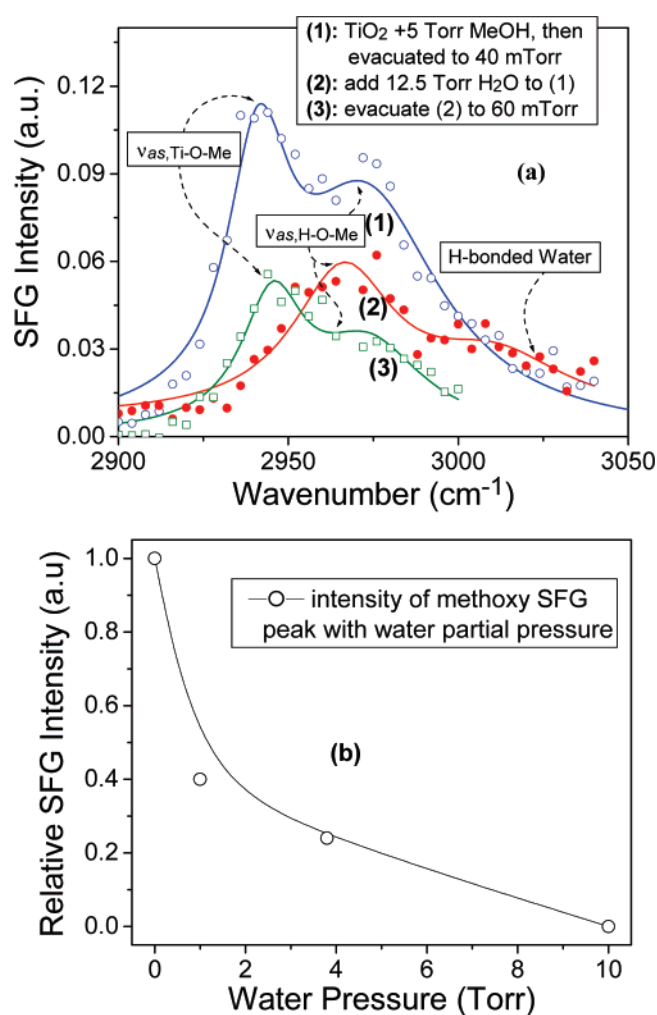


Figure 6. Evolution of the SFG resonance of methanol on TiO₂ with introduction of water vapor and subsequent evacuation (a) and the relative methoxy species SFG intensity as a function of water vapor pressure (b).

6a.3) upon removal of water by evacuation, indicating that a reversible process occurs at the surface. This reversible process will be discussed further in section 4.2.

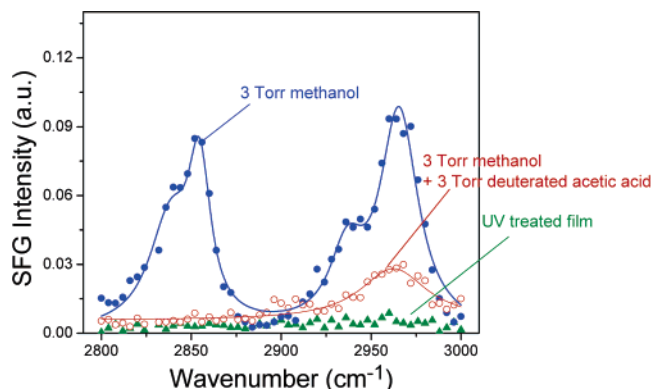


Figure 7. Evolution of the SFG spectrum of methanol on TiO₂ with the addition of acetic acid-*d*₅.

A comparison of Figures 4 and 6 shows that water has a different effect on acetic acid than on methanol adsorbed on the TiO₂ surface. Acetic acid is more strongly adsorbed on the TiO₂ surface than is methanol. The greater stability of acetic acid is shown directly by in situ SFG measurements. Figure 7 shows the result of competitive adsorption between methanol and acetic acid on TiO₂. Considering that both methanol and acetic acid contain a methyl group, the SFG CH₃ signal from methanol/methoxy and that from acetic acid interfere with each other. To avoid this interference, deuterated acetic acid (CD₃-COOD) is used in this SFG experiment. In the presence of deuterated acetic acid (Figure 7), the methoxy species SFG peaks (2828 and 2935 cm⁻¹) are eliminated. The methanol SFG peaks (2855 and 2968 cm⁻¹) are greatly diminished (by ca. 70%).

3.3. Water on TiO₂. Under ambient conditions, most metal oxide surfaces are decorated with hydroxyl groups. This is a consequence of surface water dissociative chemisorption.^{50–52} The surface hydroxyl groups on TiO₂ have been directly observed by SFG in previously reported work.⁴⁸ The SFG signal from surface hydroxyl groups is quenched by the addition of methanol.⁴⁸ We and others⁵³ have also investigated water adsorbed on the TiO₂ surfaces with and without UV treatment. Here we report the results of probing the adsorption of deuterated water (D₂O) onto the hydroxylated TiO₂ surface. As shown in Figure 8, broad SFG peaks appear in the region of 2400–2800 cm⁻¹. These peaks are due to D₂O with varying extents of hydrogen bonding and provide relative information about the water structure on the surface; the lower frequency peaks are due to more strongly H-bonded water on the surface. After 2 days of exposure to 15 Torr D₂O, the D₂O SFG signals are substantially weakened, especially on the high-frequency (2600–2800 cm⁻¹) side. This implies that this water adlayer is mobile, exchanging with H₂O, corresponding to a physisorption mode.

4. Discussion

4.1. Adsorption Isotherm and Thermodynamic Analysis of Acetic Acid on TiO₂. An adsorption isotherm reflects the relationship between the equilibrium surface and bulk concen-

- (50) Harris, L. A.; Quong, A. A. *Phys. Rev. Lett.* **2004**, *93*, 086105-1–086105-4.
 (51) Brookes, I. M.; Muryn, C. A.; Thornton, G. *Phys. Rev. Lett.* **2001**, *87*, 266103-1–266103-4.
 (52) Schaub, R.; Thosttrup, R.; Lopez, N.; Laegsgaard, E.; Stensgaard, I.; Norskov, J. K.; Besenbacher, F. *Phys. Rev. Lett.* **2001**, *87*, 266104-1–266104-4.
 (53) Uosaki, K.; Yano, T.; Nihonyanagi, S. *J. Phys. Chem. B* **2004**, *108*, 19086–19088.

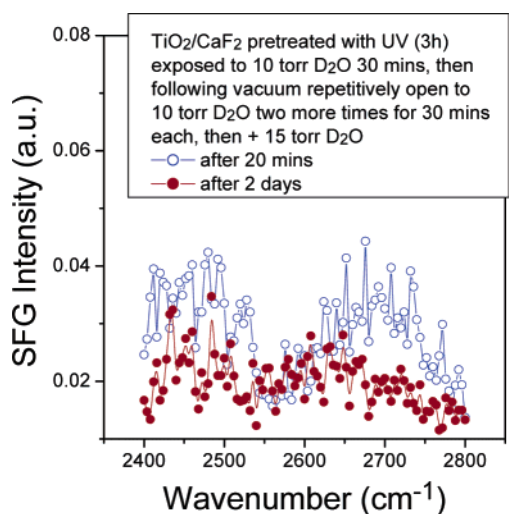


Figure 8. Evolution of the SFG spectrum of D₂O on TiO₂ with time.

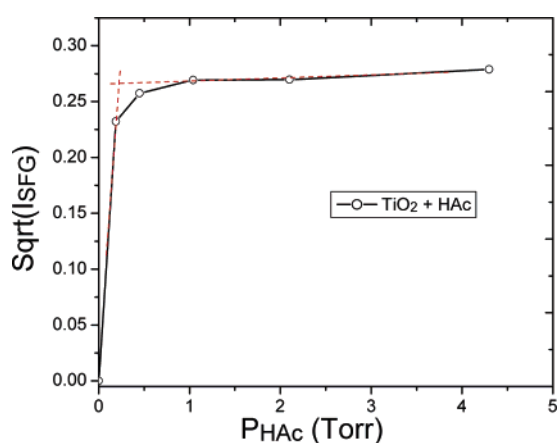


Figure 9. Square root SFG intensity for acetate on TiO₂ vs acetic acid partial pressure (room temperature).

trations.⁴⁹ Thus, to obtain an adsorption isotherm, the surface-adsorbed species must be quantified in the presence of its bulk counterpart. As a second-order nonlinear process, SFG is intrinsically surface sensitive, and thus able to measure surface-bound species without interference from the bulk.

The resonant SFG signal intensity is proportional to the square of the number of molecules contributing to the signal and to their average orientation:

$$I_{\text{SFG}} \propto |\chi^{(2)}|^2 = N^2 |\langle \beta \rangle|^2 \quad (5)$$

An adsorption isotherm can thus be obtained by determining the square root of the SFG intensity for the adsorbed acetic acid as a function of acid partial pressure. (The spectra are shown in Figure 2.) As shown in Figure 9, up to ~4.3 Torr, the surface coverage shows a monotonic increase with acetic acid partial pressure. A “knee” appears at a pressure of ca. 0.24 Torr (Figure 9), indicating the formation of a monolayer. This inflection point reflects the density of active sites available on the surface. The plateau at higher pressure signifies approach to surface saturation.

The shape of the curve shown in Figure 9 suggests a typical Langmuir adsorption mode. A Langmuir mode of gas adsorbed on a solid surface obeys⁴⁹

$$\theta = \frac{N}{N_{\text{max}}} = \frac{K(T)P}{1 + K(T)P} \quad (6)$$

where θ is the fractional surface coverage, N is the molecular coverage or density as defined before (molecules cm⁻²), N_{max} is the molecular coverage at saturation, and P is the vapor pressure of the adsorbate. $K(T)$ is the temperature-dependent Langmuir adsorption constant that describes partitioning between molecules in the gas-phase and those adsorbed on the surface.

Rearranging eq 6 in combination with the relationship between surface molecular density and the SFG signal (eq 5), one obtains

$$\frac{1}{\sqrt{I_{\text{SFG}}}} = \frac{1}{\sqrt{I_{\text{SFG,max}}}} + \frac{1}{K(T)\sqrt{I_{\text{SFG,max}}}} \frac{1}{P} \quad (7)$$

The relationship between the inverse square root of the acetic acid SFG intensity and the acetic acid partial pressure is shown in Figure 10. A least-squares fit of the data in Figure 10 results in a chemisorption constant at room temperature for the measured pressure range, $K(T = 298 \text{ K}) = (9.21 \pm 0.71) \times 10^3$. This value is much larger than that for methanol chemically adsorbed on TiO₂: 2.13×10^3 .²²

The Gibbs free energy is related to the adsorption equilibrium constant as

$$\Delta G^\circ = -RT \ln K \quad (8)$$

Substituting the value of $K(T = 298 \text{ K})$ obtained from the SFG measurement, the corresponding adsorption free energy ΔG° for acetic acid on TiO₂ is $-22.6 \pm 0.2 \text{ kJ mol}^{-1}$.

To determine the heat of adsorption or binding energy from ΔG requires either knowledge of or estimation of the corresponding entropy change. (For a detailed derivation of the entropy change, see the Supporting Information.) Upon adsorption, acetic acid is strongly bonded to the TiO₂ surface (in a bidentate configuration as reported in the literature^{9,37}), and three degrees of translational and rotational freedom are thereby lost. Applying the molecular partition function Q ,⁵⁴ the change in entropy due to the loss of translational and rotational degrees of freedom upon adsorption is calculated, $\Delta S_{\text{ads,trans+rot}} = -(159.95 + 100.02) \approx -260 \text{ J mol}^{-1} \text{ K}^{-1}$. In addition, the molecular configuration on the surface also contributes to the entropy change. However, on average, surface configurational entropy is negligibly small compared to translational and rotational entropy.

Combining the experimental free energy and estimated adsorption entropy, the heat of adsorption or binding energy (i.e., negativity of the enthalpy of adsorption) for acetic acid adsorbed on the TiO₂ surface,

$$-\Delta H^\circ = -(\Delta G^\circ + T\Delta S^\circ) \quad (9)$$

$-\Delta H^\circ$ is $99.58 \text{ kJ mol}^{-1}$ at 298 K. This value of $-\Delta H^\circ$ is consistent with chemisorption. For physisorption, the adsorption energy is normally less than 30 kJ mol^{-1} .⁵⁵ Note that this value of $-\Delta H^\circ$ is an upper limit, since a small positive contribution by molecular surface configuration is neglected in estimating

(54) McQuarrie, D. A.; Simon, J. D. *Physical chemistry: a molecular approach*; University Science Books: Sausalito, CA, 1997.

(55) Kolasinski, K. *Surface science: foundations of catalysis and nanoscience*; Wiley: Chichester, 2001.

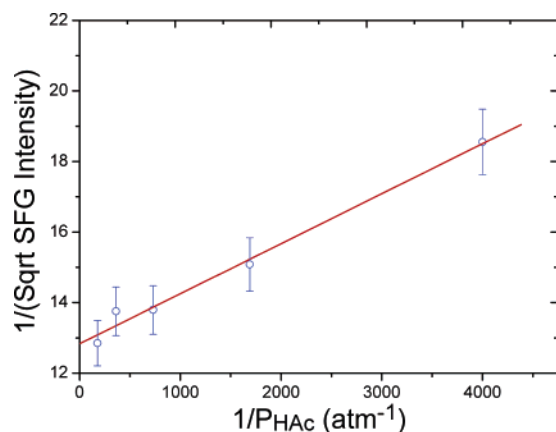


Figure 10. Relationship between the inverse square root of the SFG intensity and the inverse acetic acid partial pressure.

the adsorption entropy and the small contribution from molecule–surface vibration/libration has been neglected, too.

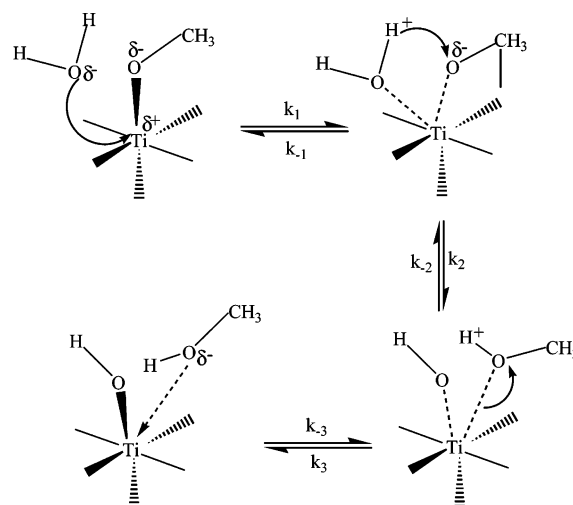
4.2. Reversible Hydroxylation and Dehydroxylation Involving Methanol and Methoxy Species. Water is ubiquitous in nature, affecting the interaction of many species with surfaces. A comparison of Figures 4 and 6 shows that water has a different effect on the adsorption of acetic acid than on the adsorption of methanol on the TiO₂ surface. The adsorption of acetic acid is essentially unaffected by the presence of water (Figure 4), indicating that acetic acid is very strongly bonded to the TiO₂ surface. In contrast, methanol adsorption (Figure 6) shows a reversible hydroxylation/dehydroxylation.

Neat methanol vapor in contact with the TiO₂ film (Figure 6a.1) results in two species: molecular methanol and a methoxy species. The two SFG peaks located at 2940 and 2970 cm⁻¹ are assigned to the methoxy species and molecular methanol, respectively. These assignments are supported by the change of SFG signals with both temperature and pressure.²² After evacuation, the methoxy species and methanol SFG signatures correspond to a submonolayer coverage.²²

When a relatively large amount of water vapor is introduced into the system (the ratio between water and methanol is ca. 300), as seen in Figure 6a,b, the surface methoxy species signal drops below the SFG detection limit, but physisorbed methanol remains, as evidenced by an appreciable SFG signal. In addition, a new broad peak beyond 3000 cm⁻¹ corresponding to H-bonded OH groups appears. The disappearance of the methoxy species SFG peak, in conjunction with the appearance of the H-bonded OH peak, indicates that the methoxy species on TiO₂ is hydrolyzed by the addition of water.

Re-evacuating the system causes the water SFG peak to drop below the SFG detection limit. The methanol peak remains. Interestingly, a substantial methoxy species SFG peak reappears (Figure 6a.3). The disappearance of water, but not of methanol, indicates that methanol is much more strongly adsorbed to the TiO₂ surface than is water. The reappearance of the methoxy species SFG peak suggests the following: (1) the methoxy species is hydrolyzed upon water addition; (2) the produced methanol remains as an adsorption layer close to or attached to the TiO₂ surface; and (3) surface dehydroxylation by methanol occurs when evacuation of the system reduces the relative water concentration, restoring the chemisorbed methoxy species on the TiO₂ surface.

Scheme 1. Reversible Hydroxylation/Dehydroxylation at the TiO₂ Surface



A reversible reaction model is proposed (Scheme 1) to explain the change in the methoxy species SFG peak in the sequence Figure 6a.1 → 6a.2 → 6a.3. Note that surface dehydroxylation by methanol, the reverse reaction, is thermodynamically favored. However, an excess of water shifts the equilibria toward the hydrolysis of the surface methoxy species.

4.3. Comparison of Acetic Acid, Methanol, and Water Adsorption. In the literature,^{31,32} formic acid (HCOOH) has been documented as dissociating on *rutile* TiO₂. Formate binds to two surface Ti cations in a bridging configuration. This is experimentally confirmed by scanning tunneling microscopy images^{33,34} and X-ray photoelectron diffraction³⁵ and is theoretically supported by ab initio slab calculations.^{19,36} So the adsorption mode of carboxylic acid on *rutile* appears to be well agreed upon.

In contrast, contradictory observations have been reported for carboxylic acid adsorption on the *anatase* TiO₂ surface. Earlier TPD measurements on anatase powders suggested both molecular and dissociative adsorption of HCOOH.⁵⁶ However, more recent results from in situ STM, LEED, XPS, and TPD measurements suggest that there is only dissociative adsorption of carboxylate on anatase TiO₂ (001).^{9,37}

The present SFG study supports a single adsorption mode for acetic acid adsorbed on the anatase TiO₂ surface. Under the present experimental conditions, the anatase nanoparticulate TiO₂ film surface is hydroxylated. When acetic acid adsorbs on the TiO₂ surface (Figure 1), only one sharp SFG peak appears in the C–H region, supporting a model with only one adsorption mode. The adsorption is highly stable, with no detectable change over 2 days. The adsorbed species is unaffected either by evacuation or by addition of water (Figures 3 and 4). These SFG results suggest a chemical adsorption mode.

In contrast to the single adsorption mode observed for acetic acid, two adsorption modes—two pairs of SFG peaks in the C–H region—are observed for methanol. The two pairs of methanol peaks are stable with time (Figure 5) but have different responses to addition of water and subsequent evacuation, supporting the conclusion that there are two different adsorption modes. A model consisting of two adsorption modes is

(56) Kim, K. S.; Barteau, M. A. *Langmuir* **1988**, *4*, 945–953.

consistent with the previously reported isotherms and temperature dependence results.²²

Water adsorbed on TiO₂ produces broad SFG peaks due to hydrogen bonding with a variety of organized structures (Figure 8). The SFG peaks vary with time, suggesting that water is physically adsorbed on the TiO₂ surface. Note that physisorption is in addition to chemisorbed water: hydroxyl groups on the TiO₂ surface are also observed with SFG,⁴⁸ confirming water chemisorption on TiO₂. Both the hydroxyl and the physisorbed water SFG signals are diminished upon addition of methanol.

The present work focuses on competitive adsorption among the three probe molecules. Acetic acid has the strongest interaction with the TiO₂ surface. This is determined by the following three SFG observations. First, both methoxy species and methanol SFG peaks are quenched in the presence of acetic acid with the same partial pressure as that of methanol (Figure 7). This indicates that acetic acid is adsorbed on the TiO₂ surface in preference to either methanol or the methoxy species. Second, the chemisorption constant for acetic acid is more than 4 times larger than that for the methoxy species.²² Third, water has little effect on the acetic acid adsorption; i.e., no noticeable change in the SFG signal is observed upon addition of water. However, hydroxylation occurs when water is added to methoxy species.

Note that the methanol and methoxy species SFG signals are eliminated only when a relatively large amount of water (the ratio of partial pressures between methanol and water is ca. 1:300; see Figure 6b) is present. In contrast, surface hydroxyl SFG signals are quenched when a low pressure of methanol is added, as previously reported.⁴⁸ These SFG observations indicate that methanol is more strongly adsorbed to the TiO₂ surface than is water.

4.4. Implications for Mechanistic Understanding of TiO₂ Photocatalysis. SFG observations concerning the relative adsorption strength of the three probe molecules have direct implications for understanding the mechanism of TiO₂-based photocatalysis, a most promising technology for environmental remediation.⁵⁷ Two mechanisms have been proposed for the TiO₂ photooxidation of organic contaminants: (1) direct oxidation by photogenerated holes,^{58,59} and (2) indirect oxidation via interfacial •OH radicals that are products of trapping valence holes by surface OH groups or adsorbed water.^{60,61} It is still a challenge to distinguish the two mechanisms due to the lack of suitable probe techniques.

For photooxidation of methanol by TiO₂, a prototype reaction toward understanding the mechanism of TiO₂ photocatalysis, the present SFG results suggest that indirect oxidation by •OH radicals is the predominant mechanism when water is the dominant species; the critical mole ratio between water and methanol for the •OH radical mechanism is about 300 (see Figure 6b).⁴⁸ Such a high ratio applies to photooxidation of methanol by TiO₂ in aqueous systems. If the water vapor pressure is lower than the critical one, direct oxidation of methanol by photogenerated holes occurs at the TiO₂ surface.

In competition with water, acetic acid is overwhelmingly adsorbed. Direct oxidation of acetic acid by photogenerated holes is thus the prevalent pathway. This agrees well with recent kinetic modeling results for the photooxidation of formic acid at illuminated TiO₂ in aqueous suspensions, as reported by Villarreal et al.²⁹

SFG observations on the adsorption differences among the three probe molecules also shed light on TiO₂ surface modification. Surface modifications play a key role in functionalizing materials to meet specific requirements in various applications. For example, in application of TiO₂ for energy conversion in photoelectrochemical solar cells, the TiO₂ electrode surface is often sensitized with dyes to extend its spectral response to the visible range, hence making fuller use of the solar spectrum. For a good sensitization, the dye molecules must be bonded to the TiO₂ surface robustly to withstand competitive adsorption from other molecules, e.g., water. The in situ SFG observations suggest that dyes with carboxyl groups are advantageous in this scenario. It has been found that the electron injection efficiency to a TiO₂ substrate from a dye with four carboxylic groups is four times as high as that from a similar dye with one carboxylic group.²⁵

Additionally, surface modifications also play a critical role in nanomaterial synthesis and assembly. To obtain materials with controlled size, surface passivation is often incorporated in the synthesis protocol. On the basis of the SFG observations herein reported, passivating agents with carboxyl groups are expected to be particularly effective in the synthesis of TiO₂-based nanomaterials. The same principle applies to nanomaterial assembly. In recent years, nanomaterial assembly has focused on maximizing the materials function by assembling specific structures.^{62,63} It is critical to find a suitable linking agent for the assembly. The present SFG results suggest that agents with a carboxylic group would be effective for assembling TiO₂ with other materials.

5. Conclusions

The adsorption of three probe molecules—acetic acid, methanol, and water—on a nanoparticulate anatase TiO₂ film surface has been studied using in situ SFG with an emphasis on adsorption modes, stabilities, and the competition among the three molecules.

Evolution of the SFG signal with time, evacuation, and addition of water demonstrates that for acetic acid on an anatase TiO₂ surface there is only one adsorption mode: chemisorption. The Langmuir constant for the chemisorption at room temperature is ca. $(9.21 \pm 0.71) \times 10^3$.

Two modes are observed for methanol adsorbed on TiO₂: chemisorption and physisorption. These two adsorption modes are relatively stable over time but show different responses to addition of water and subsequent evacuation. When water is present, methanol/methoxy are involved in a reversible hydroxylation/dehydroxylation at the TiO₂ surface.

The in situ SFG study unambiguously resolves the competitive adsorption among the three molecules: acetic acid, methanol, and water. The adsorption strength follows the order acetic acid (strongest), methanol, water (weakest). The adsorp-

(57) Hoffmann, M. R.; Martin, S. T.; Choi, W. Y.; Bahnemann, D. W. *Chem. Rev.* **1995**, *95*, 69–96.

(58) Chen, J.; Ollis, D. F.; Rulkens, W. H.; Bruning, H. *Water Res.* **1999**, *33*, 669–676.

(59) Bahnemann, D. W.; Hilgendorff, M.; Memming, R. *J. Phys. Chem. B* **1997**, *101*, 4265–4275.

(60) Wang, C. Y.; Rabani, J.; Bahnemann, D. W.; Dohrmann, J. K. *J. Photochem. Photobiol. A—Chem.* **2002**, *148*, 169–176.

(61) Wang, C. Y.; Pagel, R.; Bahnemann, D. W.; Dohrmann, J. K. *J. Phys. Chem. B* **2004**, *108*, 14082–14092.

(62) Li, L. S.; Hui, Z.; Chen, Y. M.; Zhang, X. T.; Peng, X. G.; Liu, Z. F.; Li, T. J. *J. Colloid Interface Sci.* **1997**, *192*, 275–280.

(63) Rajh, T.; Thurnauer, M. C.; Thiagarajan, P.; Tiede, D. M. *J. Phys. Chem. B* **1999**, *103*, 2172–2177.

tion strength and different responses of methanol and of acetic acid adsorption to water addition have direct implications to practical applications of TiO₂-based materials.

Acknowledgment. Financial support by the National Science Foundation (No. CHE-9816380) is gratefully acknowledged.

Supporting Information Available: Approximation of adsorption entropy for acetic acid on TiO₂. This material is available free of charge via the Internet at <http://pubs.acs.org>.

JA051996M